Polyhedron 90 (2015) 165–174

Contents lists available at ScienceDirect

Polyhedron

journal homepage: www.elsevier.com/locate/poly

Hydrogen bond networks in five- and eight-membered palladium and platinum complexes derived from *bis*(2-aminophenyl)ether and *bis*(2-aminophenyl)thioether ligands

Uvaldo Hernández-Balderas [a], Noemí Andrade-López [a,*], José G. Alvarado-Rodríguez [a], Rafael Moreno-Esparza [b], Margarita Paneque [c]

[a] *Centro de Investigaciones Químicas, Universidad Autónoma del Estado de Hidalgo, Ciudad Universitaria, Carretera Pachuca–Tulancingo km 4.5, Colonia Carboneras, Mineral de la Reforma, Hgo. C.P. 42184, Mexico*

[b] *Facultad de Química (UNAM), Ed. B. Ave. Universidad 3000, C.P. 04510, Coyoacán, México D.F., Mexico*

[c] *Instituto de Investigaciones Químicas (IIQ) and Departamento de Química Inorgánica, CSIC and Universidad de Sevilla, Av. Américo Vespucio 49, 41092 Sevilla, Spain*

ARTICLE INFO

Article history:
Received 24 October 2014
Accepted 6 February 2015
Available online 14 February 2015

Keywords:
Nitrogenate ligands
Pd and Pt complexes
X-ray diffraction
κ^2N, $\kappa N\kappa S$, and $\kappa^2N\kappa S$ modes
Noncovalent interactions

ABSTRACT

The reaction of $[\mathbf{M}^{II}(MeCN)_2Cl_2]$ ($\mathbf{M}$ = Pd, Pt) with the diamino ligands either *bis*(2-aminophenyl)ether or *bis*(2-aminophenyl)thioether $\{(NH_2\text{-}C_6H_4)_2\boldsymbol{D}\}$ [$\boldsymbol{D}$ = O ($\mathbf{L^1}$); $\boldsymbol{D}$ = S ($\mathbf{L^2}$)] yielded neutral coordination complexes of general formulae $[\mathbf{M}(\mathbf{L}^{\boldsymbol{n}})Cl_2]$ [$\mathbf{M}$ = Pd, $n = 1$ (**1**); Pt, $n = 1$ (**2**); Pd, $n = 2$ (**3**); Pd, $n = 2$ (**4**); Pt, $n = 2$ (**5**). The reaction of $\mathbf{L^2}$ with $K_2[PtCl_6]$ promoted the mono-deprotonation of the diamino ligand to yield the neutral complex $[Pt^{IV}\{(NH_2\text{-}C_6H_4)S(NH\text{-}C_6H_4)\}Cl_3]$ (**6**); when the $H_2[PtCl_6]$ acid was used an ionic complex $[Pt^{IV}(\mathbf{L^2})Cl_3]Cl$ (**7**) was obtained. All complexes were characterized by NMR in solution, vibrational spectroscopy, and by X-ray diffraction studies. The molecular structures of the complexes revealed different coordination patterns of the diamino ligands; $\mathbf{L^1}$ just displayed a κ^2N mode meanwhile $\mathbf{L^2}$ exhibited a wide variety of patterns (κ^2N, $\kappa N\kappa S$, and $\kappa^2N\kappa S$) forming chelate rings of five- or eight-members. The presence of N–H functions in the ligand moieties enhanced the formation of extended hydrogen-bond networks; these supramolecular arrangements were mainly discussed at unitary and binary levels and sorted according to the molecular coordination patterns observed.

1. Introduction

In Coordination Chemistry, nitrogenate ligands based on the chemical framework **I** have been utilized as precursors of transitional metal complexes of Ti^{II}, Zr^{II}, Zr^{IV}, Hf^{II}, Hf^{IV}, [1] Co^{II}, and Fe^{II} [2]. A number of these complexes have displayed catalytic applications in asymmetric synthesis and in alkene polymerization; this catalytic behavior has been associated with the flexibility of the molecular framework and with the nature of the donor atom present in the ligands [2–4]. From a structural point of view, a thorough analysis of a number of structures of complexes containing ligands based on the framework **I**, retrieved from the Cambridge Structural Database (version 5.35, updated February 2014), revealed that, in most of the ligands of the type **I** used, the atoms attached to the nitrogen atoms are organic groups such as substituted phenyl groups or *tert*-butyl groups in order to take advantage of their electronic and steric inherent effects. Nevertheless, the increase of these organic groups led to a concomitant decrease in the number of hydrogen atoms attached to the nitrogen atoms, reducing the ability of the molecular complexes, for example, to display N–H–acceptor interactions. In this regard, it is widely recognized that noncovalent interactions such as hydrogen- and halogen bonding play a fundamental role in the formation of supramolecular aggregates that display fascinating architectures achieved in solid state [5–8]. In particular, it has been highlighted the importance of the presence of N–H functions in platinum complexes; the presence of N–H–acceptor interactions may have a remarkable influence in the way that some platinum-based drugs select the DNA as a target in the cell [9].

Continuing with our studies of Coordination Chemistry of nitrogenate ligands with Group 10 metals [10–12] we thought worthwhile to investigate the influence of the donor atom ***D*** in the coordination mode of the ligands $\mathbf{L^1}$ and $\mathbf{L^2}$ toward palladium and platinum and the role of the N–H groups in the formation of supramolecular arrangements. To the best of our knowledge, there is just one report of the coordination studies of these ligands, in particular $\mathbf{L^1}$, with Zn^{II}; [13] in this report the analysis of the

---

* Corresponding author.
E-mail address: nandrade@uaeh.edu.mx (N. Andrade-López).

http://dx.doi.org/10.1016/j.poly.2015.02.004
0277-5387/© 2015 Elsevier Ltd. All rights reserved.

molecular structure revealed that the oxygen atom is not bound to the zinc atom and, additionally, there are just some few lines dedicated to the description of the supramolecular network based on N–H–Cl interactions. Hence, we report herein the synthesis and characterization in solution and solid state of seven complexes of palladium and platinum, Fig. 1, where the ligands displayed three coordination modes. In the solid state, the presence of either four (**1**–**5** and **7**) or three (**6**) N–H groups displayed interesting hydrogen bond networks based on rings or chains.

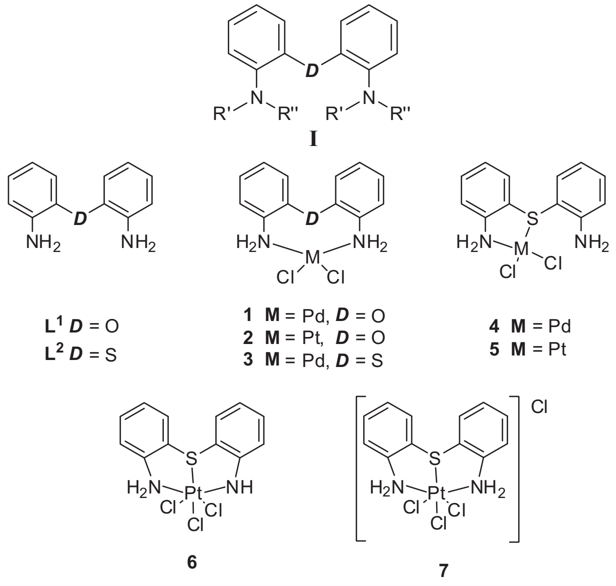

Fig. 1. Structure of complexes of palladium and platinum derived from $\mathbf{L^1}$ and $\mathbf{L^2}$ ligands.

2. Experimental

2.1. General details

All the manipulations of air and moisture sensitive materials were carried out under dinitrogen atmosphere using Schlenk techniques. Solvents such as acetone, acetonitrile (MeCN), dimethylformamide (DMF), and dimethylsulfoxide (DMSO) were dried according to the standard methods and distilled before their use. HCl (37%), $PdCl_2$, $PtCl_2$, $K_2[PtCl_6]$, and $H_2[PtCl_6]$ were purchased from Aldrich and used as received. The $[\mathbf{M}(MeCN)_2Cl_2]$ complexes (**M** = Pd, Pt) used as starting materials were prepared and isolated as reported [14]. Melting points were recorded on a Mel–Temp II apparatus and reported without correction. Elemental analyses were performed on a Perkin–Elmer Series II CHNS/O Analyzer 2400. Mass spectra were recorded by using a Bruker MicroTOF II spectrometer. Infrared spectra were recorded on a FT–IR 200 PerkinElmer spectrophotometer in the 4000–400 cm^{-1} range using KBr pellets. Raman spectra in the solid state were recorded in the 4000–100 cm^{-1} scale on a Perkin–Elmer spectrum GX NIR FT–Raman spectrophotometer with 10–280 mW laser power and 4 cm^{-1} resolution. NMR spectra were recorded on a Varian NMRS 400 spectrometer in either DMSO-d_6, acetone-d_6, DMF-d_7, or DMF–acetone d_6 mixtures (1:2). Chemicals shifts (ppm) are relative to the frequency of tetramethylsilane (TMS) with the residual protio-solvent signal used as reference for ^{1}H (399.78 MHz) and $^{13}C\{^1H\}$ (100.53 MHz). Unequivocal NMR assignments for the ligands $\mathbf{L^1}$ and $\mathbf{L^2}$ and for the complexes **1**–**7** were carried out by two–dimensional homo- and heteronuclear experiments (COSY, HSQC, and NOESY). X-ray diffraction data of **1**–**7** were collected at room temperature on an Oxford Diffraction GEMINI CCD diffractometer with either graphite-monochromated Mo Ka radiation (λ = 0.71073 Å) for **1**, **3**, **4**, and **5** or Cu Ka radiation (λ = 1.54184 Å) for **2**, **6**, and **7**. Data were integrated, scaled, sorted, and averaged using the CRYSALIS software package [15].

Using Olex2 [16], the structures were solved with the ShelXS [17] structure solution program using Direct Methods and refined with the ShelXL [17] refinement package using Least Squares minimization. All non-hydrogen atoms were refined anisotropically. The positions of the hydrogen atoms were kept fixed with a common isotropic displacement parameter. In the crystal structures of compounds **1**·DMSO, **2**·Me_2CO, and **7**·Me_2CO the solvent molecules displayed positional disorder over two positions, with the main component having occupancies of 0.8848(18), 0.545(13), and 0.55(2), respectively. In the case of **5**·Me_2CO the acetone molecule is also disordered, but is located on a crystallographic center and, consequently, was refined with its occupancy set to 0.50; the main component has an occupancy of 0.294(17). SAME, SIMU, DELU, and FLAT instructions were used during the refinement of the disorder.

2.2. Synthesis of bis(2-aminophenyl)ether ($\mathbf{L^1}$) and bis(2-aminophenyl)thioether ($\mathbf{L^2}$) ligands

In order to synthetize the ligands $\mathbf{L^1}$ and $\mathbf{L^2}$, firstly we prepared the corresponding *ortho*-dinitrocompounds $\mathbf{D}(C_6H_4\text{-}NO_2)_2$ (**D** = O, S). Thus, when **D** = O, we followed the reported method to prepare the *bis*(2-nitrophenyl)ether [18]. On the other hand, in the case of **D** = S, we mimicked the method previously described for *bis*(4-nitrophenyl)thioether [19], where we used *ortho*-chloronitrobenzene as starting material instead of the *para* compound. Then, in each case, we carried out the reduction of both $-NO_2$ functional groups by using iron powder in acidic media to prepare the diamino compounds $\mathbf{L^1}$ and $\mathbf{L^2}$ (see below).

2.2.1. General procedure for the synthesis of $\mathbf{L^1}$ and $\mathbf{L^2}$

A suspension of iron powder and HCl in water was stirred and refluxed for 25 min. Then, the corresponding dinitro compound was added to this hot suspension and the mixture was refluxed for 24 h. The mixture was allowed to reach room temperature and hydrolyzed with 20 mL of NaOH 2.5 M and, extracted with chloroform (2 × 20 mL). The organic phase was dried with Na_2SO_4 and evaporated to yield the diamino compounds as solids.

2.2.2. Synthesis of $\mathbf{L^1}$

4.30 g (76.9 mmol) of iron, 2 mL of HCl in 20 mL of water, 2.00 g (7.69 mmol) of *bis*(2-nitrophenyl)ether. Pale pinkish-orange solid. Yield: 85% (1.32 g, 6.60 mmol). M. p.: 64 °C. *Anal.* Calc. for $C_{12}H_{12}N_2O$: C, 71.98; H, 6.04. Found: C, 71.53; H, 6.31%. IR (KBr cm^{-1}) ν: = 3442, 3353 (N–H); 1621; 1495 (C=C); 1203 (C–O–C). Raman (420 mW, cm^{-1}) ν = 3342 (N–H); 3060 (C–H); 1611 (C=C); 1149, 1032 (C–O–C). ^{1}H NMR (DMF-acetone-d_6) δ = 6.85 (m, 2H, H3, H4); 6.66 (d, 1H, H6, $^3J_{H6\text{-}H5}$ = 8.31 Hz), 6.53 (dd, 1H, H5, $^3J_{H5\text{-}H6}$ = 8.31, $^3J_{H5\text{-}H4}$ = 6.85 Hz), 4.85 (s, 2H, NH_2). ^{13}C NMR (DMF-acetone-d_6) δ = 144.1 (C1), 140.1 (C2), 124.4 (C4), 118.3 (C6), 116.3 (C3), 117.3 (C5).

2.2.3. Synthesis of $\mathbf{L^2}$

4.05 g (72.5 mmol) of iron, 2 mL of HCl 1.6 M, 2.00 g (7.25 mmol) of *bis*(2-nitrophenyl)thioether. Yellow solid. Yield: 61% (0.96 g, 4.44 mmol). M. p.: 88 °C. *Anal.* Calc. for $C_{12}H_{12}N_2S$: C, 66.63; H, 5.59. Found: C, 66.85; H, 5.68%. IR (KBr cm^{-1}) ν = 3455, 3338 (N–H); 1611, 1472 (C=C). Raman (420 mW, cm^{-1}) ν = 3345 (N–H); 3060 (C–H); 1585 (C=C). ^{1}H NMR (DMF-acetone-d_6) δ = 7.12 (d, 1H, H6, $^3J_{H6\text{-}H5}$ = 7.55 Hz); 7.02 (dd, 1H, H4, $^3J_{H4\text{-}H5}$ = 7.31, $^3J_{H4\text{-}H3}$ = 7.83 Hz); 6.79 (d, 1H, H3, $^3J_{H3\text{-}H4}$ = 7.83 Hz); 6.54

(dd, 1H, H5, $^{3}J_{H5\text{-}H6}$ = 7.55, $^{3}J_{H5\text{-}H4}$ = 7.31 Hz). ^{1}H NMR (DMSO-d_6) δ = 7.08 (dd, 1H, H6, $^{3}J_{H6\text{-}H5}$ = 7.72, $^{4}J_{H6\text{-}H4}$ = 1.32 Hz); 7.01 (dd, 1H, H4, $^{3}J_{H4\text{-}H5}$ = 7.44, $^{3}J_{H4\text{-}H3}$ = 7.99 Hz); 6.72 (dd, 1H, H3, $^{3}J_{H3\text{-}H4}$ = 7.99, $^{4}J_{H3\text{-}H5}$ = 1.20 Hz); 6.50 (ddd, 1H, H5, $^{3}J_{H5\text{-}H6}$ = 7.72, $^{3}J_{H5\text{-}H4}$ = 7.44, $^{4}J_{H5\text{-}H3}$ = 1.20 Hz); 5.30 (s, 2H, NH_2). ^{13}C NMR (DMF-acetone-d_6) δ = 149.0 (C2); 133.8 (C6); 129.5 (C4); 117.8 (C5); 116.8 (C1); 115.6 (C3).

2.3. Synthesis of the palladium(II) complexes

2.3.1. General procedure

To a solution of [Pd(MeCN)$_2$Cl$_2$] in acetonitrile at 0 °C the corresponding **L^1** or **L^2** ligand was added; the reaction mixture was stirred for 24 h. Then, the solution was warmed to room temperature and the solid obtained was filtered by suction.

2.3.2. Synthesis of [Pd{κ^2N-(NH_2-C_6H_4)$_2$O}Cl$_2$] (**1**)

[Pd(MeCN)$_2$Cl$_2$] [0.065 g (0.25 mmol)], cold acetonitrile (10 mL), and **1** [0.05 (0.25 mmol)]. The yellow solid was washed with acetonitrile (2 × 3 mL). Yield: 95% (0.089 g, 0.236 mmol). Orangish-yellow single crystals of **1** were obtained from a saturated DMSO solution. M. p.: 254 °C (dec.). *Anal.* Calc. for $C_{10}H_{12}Cl_2N_2OPd\cdot C_2H_6OS$: C, 36.90; H, 3.98; N 6.15. Found: C, 36.88; H, 3.93; N, 5.78%. IR (KBr cm^{-1}) ν = 1620, 1490 (C=C); 1189 (C–O–C). Raman (420 mW, cm^{-1}) ν = 3070 (N–H); 1601 (C=C); 440 (Pd–N); 319 (Pd–Cl). ^{1}H NMR (DMF-acetone-d_6) δ = 7.83 (dd, 1H, H3, $^{3}J_{H3\text{-}H4}$ = 8.20, $^{4}J_{H3\text{-}H5}$ = 1.20 Hz); 7.25 (m, 2H, H4, H6); 7.11 (ddd, 1H, H5, $^{3}J_{H5\text{-}H6}$ = 7.80, $^{3}J_{H5\text{-}H4}$ = 7.60, $^{4}J_{H5\text{-}H3}$ = 1.20 Hz). ^{13}C{^{1}H} NMR (DMF-acetone-d_6) δ = 149.8 (C2); 136.0 (C1); 126.9 (C4); 126.7 (C5); 123.9 (C3); 123.6 (C6).

2.3.3. Synthesis of [Pd{κ^2N-(NH_2-C_6H_4)$_2$S}Cl$_2$] (**3**) and [Pd{κN,κS-(NH_2-C_6H_4)$_2$S}Cl$_2$] (**4**)

[Pd(MeCN)$_2$Cl$_2$] [0.12 g (0.46 mmol)], cold acetonitrile (10 mL), **2** [0.10 g (0.46 mmol)]. Yellow solid, Yield: 94% (0.17 g, 0.44 mmol). NMR spectra of the yellow solid displayed the formation of **3** and **4** as a mixture in a 70:30 ratio. *Anal.* Calc. for $C_{24}H_{23}Cl_4N_4Pd_2S_2$: C, 36.62; H, 3.07. Found: C, 36.05; H, 3.06%. IR (KBr cm^{-1}) ν: 3455, 3338 (N–H); 1611, 1472 (C=C). Raman (420 mW, cm^{-1}) ν = 3343 (NH); 1585 (C=C). From a saturated acetonitrile solution of the yellow solid were obtained red crystals for **3**, m. p.: 239–241 °C (dec.), and orange crystals for **4**, which do not melt below 250 °C.

Complex **3** was observed as the minor product. ^{1}H NMR (DMF-d_7) δ = 7.98 (d, 1H, H3, $^{3}J_{H3\text{-}H4}$ = 7.82 Hz), 7.37 (dd, 1H, H4, $^{3}J_{H4\text{-}H3}$ = $^{3}J_{H4\text{-}H5}$ = 7.82 Hz), 7.25 (m, 1H, H5), 7.04 (d, 1H, H6, $^{3}J_{H6\text{-}H5}$ = 8.31 Hz). ^{13}C{^{1}H} NMR (DMF-d_7) δ = 145.5 (C2), 137.5(C6), 131.5 (C4), 126.5 (C3), 123.8 (C5), 122.0 (C1). **4** (main compound). ^{1}H NMR (DMF-d_7) δ = 7.60 (m, 4H, H3, H4, H6, H12), 7.48 (dd, 1H, H5, $^{3}J_{H5\text{-}H6}$ = $^{3}J_{H5\text{-}H4}$ = 7.34 Hz), 7.25 (m, 2H, H10), 6.94 (d, 1H, H9, $^{3}J_{H9\text{-}H10}$ = 7.82 Hz), 6.65 (dd, 1H, H11, $^{3}J_{H11\text{-}H12}$ = 7.82, $^{3}J_{H11\text{-}H10}$ = 7.34 Hz). ^{13}C{^{1}H} NMR (DMF-d_7) δ = 149.5 (C8), 145.6 (C2), 135.4 (C12), 132.8 (C10), 132.5 (C1), 131.7 (C4), 131.6 (C6), 129.5 (C5), 131.5 (C3), 118.0 (C9), 117.3 (C11), 113.8 (C7).

2.4. Synthesis of the platinum(II) complexes

2.4.1. General procedure

To a solution of [Pt(MeCN)$_2$Cl$_2$] in hot acetonitrile (80 °C) the corresponding **L^1** or **L^2** ligand was added; the reaction mixture was stirred for 72 h in the case of **2**, and 24 h for **5**. Then, the solution was cooled to room temperature and the solid obtained was filtered by suction.

2.4.2. Synthesis of [Pt{κ^2N-(NH_2-C_6H_4)$_2$O}Cl$_2$] (**2**)

[Pt(MeCN)$_2$Cl$_2$] [0.08 g (0.30 mmol)], hot acetonitrile (10 mL), **1** [0.06 g (0.30 mmol)]. Yield: 74% (0.08 g, 0.22 mmol). M. p.: 176 °C (dec.). Yellow single crystals of **2** were obtained from a saturated acetone solution. *Anal.* Calc. for $C_{12}H_{12}Cl_2N_2OPt\cdot 1.3CH_3CN$: C, 33.81; H, 3.10. Found: C, 33.71; H, 3.34%. ESI-HRMS: calcd. for $C_{12}H_{12}Cl_2N_2NaOPt$ [M+Na]$^+$ 487.9867; found 488.9865; error 3.1 ppm. IR (KBr cm^{-1}) ν = 1592, 1490 (C=C); 1209 (C–O–C). Raman (420 mW, cm^{-1}) ν = 3,085 (C–H); 1603 (C=C); 1227 (C–O–C); 324 (Pt–Cl). ^{1}H NMR (DMF-acetone-d_6) δ = 7.83 (d, 1H, H3, $^{3}J_{H3\text{-}H4}$ = 8.06 Hz); 7.25 (m, 2H, H4, H6); 7.60 (s, br., 2H, NH_2), 7.12 (dd, 1H, H5, $^{3}J_{H5\text{-}H6}$ = 8.00, $^{3}J_{H5\text{-}H4}$ = 7.25 Hz). ^{13}C{^{1}H} NMR (DMF-acetone-d_6) δ = 150.1 (C2); 136.5 (C1); 126.8 (C4); 126.6 (C5); 123.7 (C3); 123.6 (C6).

2.4.3. Synthesis of [Pt{κN,κS-(NH_2-C_6H_4)$_2$S}Cl$_2$] (**5**)

[Pt(CH_3CN)$_2$Cl$_2$] [0.10 g (0.29 mmol)], acetonitrile (20 mL), **2** [0.062 g (0.29 mmol)]. Yield: 92% (0.13 g, 0.26 mmol). M. p.: 244 °C (dec.). Green crystals from a saturated acetone solution of **5** were obtained. ESI-HRMS: calcd. for $C_{12}H_{12}ClN_2PtS$ [M−Cl+1]$^+$ 446.00521, found 516.9418, error 2.5 ppm. IR (KBr cm^{-1}) ν = 3440, 3146 (N–H); 1618, 1480 (C=C). ^{1}H NMR (DMF-acetone-d_6) δ = 8.66 (s, br., 2H, NH_2), 8.24 (s, br., 2H, NH_2), 7.65 (d, 1H, H3, $^{3}J_{H3\text{-}H4}$ = 7.80 Hz); 7.61 (dd, 1H, H12, $^{3}J_{H12\text{-}H11}$ = 7.94, $^{4}J_{H12\text{-}H10}$ = 1.27 Hz); 7.52 (dd, 1H, H6, $^{3}J_{H6\text{-}H5}$ = 7.88, $^{4}J_{H6\text{-}H4}$ = 1.00 Hz); 7.43 (ddd, 1H, H4, $^{3}J_{H4\text{-}H5}$ = 7.57, $^{3}J_{H4\text{-}H3}$ = 7.80, $^{4}J_{H4\text{-}H6}$ = 1.12 Hz); 7.33 (ddd, 1H, H5, $^{3}J_{H5\text{-}H4}$ = 7.57, $^{3}J_{H5\text{-}H6}$ = 7.88, $^{4}J_{H5\text{-}H3}$ = 1.00 Hz); 7.19 (ddd, 1H, H10, $^{3}J_{H10\text{-}H11}$ = 7.65, $^{3}J_{H10\text{-}H9}$ = 8.13, $^{4}J_{H10\text{-}H12}$ = 1.30 Hz); 6.86 (dd, 1H, H9, $^{3}J_{H9\text{-}H10}$ = 8.13, $^{4}J_{H9\text{-}H11}$ = 1.00 Hz); 6.62 (ddd. 1H, H11, $^{3}J_{H11\text{-}H10}$ = 7.65, $^{3}J_{H11\text{-}H12}$ = 7.94, $^{4}J_{H10\text{-}H12}$ = 1.00 Hz). ^{13}C{^{1}H} NMR (DMF-acetone-d_6) δ = 149.3 (C8); 146.6 (C2); 135.5 (C12); 134.6 (C1); 133.3 (C10); 131.9 (C4); 131.3 (C6); 130.0 (C5); 127.2 (C3); 117.6 (C11); 117.5 (C9); 112.8 (C7).

2.5. Synthesis of the platinum(IV) complexes

2.5.1. Synthesis of [Pt{κ^2N,κS-(NH_2-C_6H_4)S(NH-C_6H_4)}Cl$_3$] (**6**)

A mixture of $K_2[PtCl_6]\cdot 6H_2O$ (0.112 g, 0.230 mmol) and **2** (0.050 g, 0.230 mmol) in 10 mL of methanol was refluxed for 30 min, then 4 mL of water were added. The solution was refluxed for 30 min and then cooled to room temperature; the suspension was filtered by suction and the brown solid obtained was washed with acetone (3 × 5 mL). On the other hand, the filtered MeOH/water solution was dried with Na_2SO_4 and evaporated to dryness, yielding a brown solid. Overall, the yield of the brown solid was 35% (0.042 g, 0.081 mmol). M. p.: 134–136 °C (dec.). From a saturated acetone solution were obtained brown crystals of **6**. *Anal.* Calc. for $C_{12}H_{11}Cl_3N_2SPt\cdot C_3H_6O$: C, 31.34; H, 2.98. Found: C, 31.38; H, 2.98%. IR (KBr cm^{-1}) ν: 2921 (C–H); 1537, 1479 (C=C). ^{1}H NMR (acetone-d_6) δ = 8.08 (d, 1H, H3, $^{3}J_{H3\text{-}H4}$ = 8.07 Hz); 7.47 (d, br., 1H, H6, $^{3}J_{H6\text{-}H5}$ = 7.45 Hz); 7.32 (dd, 1H, H5, $^{3}J_{H5\text{-}H6}$ = 7.45, $^{3}J_{H5\text{-}H4}$ = 7.68 Hz); 7.15 (t, vbr., 1H, H4). ^{13}C{^{1}H} NMR (acetone-d_6) δ = 133.3 (C5); 131.5 (C3); 126.3 (vbr., C6); not observed (C1, C2, and C4).

2.5.2. Synthesis of [Pt{κ^2N,κS-(NH_2-C_6H_4)$_2$S}Cl$_3$]Cl (**7**)

2 (0.063 g, 0.290 mmol) was added to a solution of $H_2[PtCl_6]\cdot 6H_2O$ (0.150 g, 0.290 mmol) in 10 mL of methanol at room temperature. The mixture was stirred for 24 h; then, the suspension was filtered and the yellow solid obtained was washed with acetone (2 × 5 mL). Yield 79% (0.127 g, 0.230 mmol). M. p.: 149 °C (dec.). From a saturated acetone solution of **7** were obtained yellow crystals. ESI-HRMS: calcd. for $C_{12}H_{12}Cl_3N_2PtS$ [M]$^+$ 515.9429, found 516.9418, error 2.5 ppm. IR (KBr cm^{-1}) ν: 2, 750 (N–H_2^+); 1,547, 1,478 (C=C). ^{1}H NMR (DMF-acetone-d_6) δ = 8.51 (d, 1H, H3, $^{3}J_{H3\text{-}H4}$ = 7.67 Hz); 7.73 (d, 1H, H6, $^{3}J_{H6\text{-}H5}$ = 7.64 Hz); 7.59 (dd, 1H, H5, $^{3}J_{H5\text{-}H6}$ = 7.64, $^{3}J_{H5\text{-}H4}$ = 7.20 Hz); 7.52 (t, vbr., 1H, H4), 3.70 (s, br., 2H, NH_2). ^{1}H NMR (DMF-acetone-d_6, 40 °C) δ = 8.52 (d, 1H, H3, $^{3}J_{H3\text{-}H4}$ = 8.00 Hz); 7.76 (d, 1H, H6, $^{3}J_{H6\text{-}H5}$ = 8.00 Hz); 7.60

(dd, 1H, H5, $^3J_{H5\text{-}H6}$ = 8.00, $^3J_{H5\text{-}H4}$ = 7.20 Hz); 7.53 (dd, 1H, H4, $^3J_{H4\text{-}H3}$ = 7.60, $^3J_{H4\text{-}H5}$ = 7.20 Hz); 3.86 (s, br., 2H, NH_2), $^{13}C\{^1H\}$ NMR (DMF-acetone-d_6) δ = 134.3 (C5); 132.4 (C3); 130.5 (vbr., C4); 127.6 (vbr., C6); not observed (C1, and C2). $^{13}C\{^1H\}$ NMR (DMF-acetone-d_6, 40 °C) δ = 146.6 (br., C2); 133.5 (C5); 131.6 (C3); 129.5 (br., C4); 126.8 (C6); 117.1 (br., C1).

3. Results and discussion

3.1. Synthesis of the Pd^{II} and Pt^{II} complexes **1** and **2** derived from $\mathbf{L^1}$

Complexes **1** and **2** were obtained from the reaction of the ligand $\mathbf{L^1}$ with [**M**(MeCN)$_2$Cl$_2$] (**M** = Pd, Pt) in an equimolar ratio, see Scheme 1. Complexes **1** and **2** were obtained as air-stable solids, moderately soluble in DMSO, DMF, and in a DMF-acetone mixture. In DMSO solution, **1** tends to yield unidentifiable products.

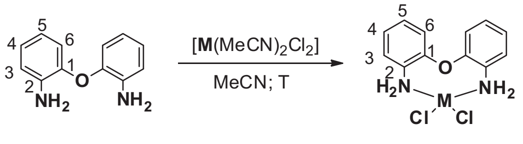

$\mathbf{L^1}$

1 **M** = Pd; T = 0 °C

2 **M** = Pt; T = 80 °C

Scheme 1. Synthesis of the Pd^{II} and Pt^{II} complexes derived from $\mathbf{L^1}$. (Numbering scheme for NMR is shown.)

3.2. Synthesis of the metallic complexes derived from $\mathbf{L^2}$ (**3–7**)

Complexes **3**–**5** were synthesized from the reaction of $\mathbf{L^2}$ with [**M**(MeCN)$_2$Cl$_2$] (**M** = Pd, Pt) in an equimolar ratio. For the formation of **6** the salt $K_2[PtCl_6]$ was used; the acid $H_2PtCl_6{\cdot}6H_2O$ was used for the synthesis of **7**, see Scheme 2. The complexes **3** and **4** were observed as a mixture of linkage isomers in a 30:70 ratio (see below). The complexes were obtained as air-stable solids, moderately soluble in acetone, DMF, and DMF-acetone mixtures. The complexes **5** and **6** were not stable in DMSO solutions; **6** also showed the slow formation of unidentifiable products in a DMF-acetone mixture.

3.3. X-ray diffraction

Suitable crystals of compounds **1**–**7** were grown from slow evaporation at room temperature of solutions of several organic solvents. Complexes **1** and **3** were crystallized as DMSO and MeCN solvates, respectively; **2**, **5**, **6**, and **7** were obtained as acetone solvates. In the asymmetric unit of **1**, **2**, **5**, and **7** the solvents molecules are disordered over two positions. Crystallographic data are displayed in Table 1 and selected bond lengths and angles are given in Table 2.

3.3.1. Molecular structures of **1**–**7**

For the sake of the analysis, the complexes can be sorted in three sets, based upon the coordination pattern of the $\{(NH_2\text{-}C_6H_4)_2\boldsymbol{D}\}$ ligand [$\boldsymbol{D}$ = O ($\mathbf{L^1}$), S ($\mathbf{L^2}$)] as well as on the coordination number of the metallic center **M**. The first set is formed by the four-coordinate compounds **1**, **2**, and **3** with a κ^2*N* dicoordinate mode of the corresponding diaminic ligand, Fig. 2; in the second one are collected the four-coordinate compounds **4** and **5** with a κ*N*,κ*S* dicoordinate mode of $\mathbf{L^2}$, Fig. 3. In these two sets the local geometry of the **M**^{II} center is described as square planar, with a *cis* arrangement of the two chloro ligands attached to it.

For these sets, as can be observed from the listed data in the Table 2, the N–M^{II} distances in the compounds **1**–**5** are essentially the same. Moreover, these distances are also similar to other previously reported for complexes containing either [**M**(NH$_2$)$_2$Cl$_2$] or [**M**(NH$_2$)SCl$_2$] cores (**M** = Pd, Pt). In this vein, in the Figs. 1S and 2S of the Supplementary Material are plotted some structural features such as **M**–Cl, **M**–N, and **M**–S bond distances and Cl–**M**–Cl bond angles for similar Pd and Pt complexes retrieved from a search in the Cambridge Structural Database; from these structural data we calculated the average distances $d_{\mathbf{M}\text{–Cl}}$ = 2.305 Å, $d_{\mathbf{M}\text{–N}}$ = 2.051 Å, $d_{Pd\text{–}S}$ = 2.259 Å, and $d_{Pt\text{–}S}$ = 2.214 Å, average distances that agree with the data displayed in the Table 2 for the title complexes herein reported. In particular, the close similitude of the Pd–Cl and Pt–Cl bond distances in the isostructural complexes **1** and **3** can be attributed to the lanthanide contraction effect present in the 5*d* platinum(II) cation.

In addition, the analysis of the molecular structures indicates that in **1**–**3** the eight-membered chelate ring [$\boldsymbol{D}$(C$_2$N)$_2$M] has a boat–chair conformation; in **4** and **5** the five-membered chelate ring displays a planar conformation, as expected for a more constrained ring with a smaller bite. The main difference in these compounds is the absence of $\boldsymbol{D}$–M^{II} bonding in the first set of compounds while in the second one that bonding is present. It is noteworthy that we observed compounds where the ligand $\mathbf{L^1}$ only promotes the formation of compounds without O–M^{II} bonding, while the $\mathbf{L^2}$ ligand containing sulfur as donor atom can coordinate in two fashions either with or without S–M^{II} bonding, i.e., this ligand displays κ*N*,κ*S* or κ^2*N* coordination modes, respectively. Thus, the absence of *O*-coordination can be attributable to the harder nature of the oxygen atom; on the other hand, the softer sulfur atom can bind to soft acids such as palladium and platinum, allowing the formation of compounds such as **4** and **5**. Moreover, in these compounds the κ*N*,κ*S* coordination mode of $\mathbf{L^2}$ is cooperatively strengthened by a weak intramolecular hydrogen bonding Cl–H–N where the interatomic Cl–N distances are slightly longer than the van der Waals radii sum [3.460(4) Å for **4** and 3.532(4) Å for **5**; Σr_{vdW}(N, Cl) = 3.30 Å]. To achieve this hydrogen bonding, the non-coordinated $NH_2\text{-}C_6H_4$ had twisted around the S-C7 bond, where the smaller Pd-S-C7-C8 torsion angle observed for **4** agreed with the shorter N–Cl distance [105.4(2)° for **4** and 107.2(2)° for **5**].

Lastly, the third set contains the octahedral hexa-coordinate compounds **6** and **7**, where $\mathbf{L^2}$ coordinates the Pt^{IV} atom in a *facial* κ^2*N*,κ*S* tricoordinate mode, Fig. 4. A remarkable difference in these compounds is their coordination entity type; in **6** the coordination entity is neutral, where the short N–Pt^{IV} bond is essentially covalent [2.015(4) and 2.063(4) Å for N(1)–Pt and N(2)–Pt, respectively]. On the other hand, **7** has a cationic entity with N–Pt distances significantly similar and a chloride acting as an anion. The S–Pt^{IV} distances are very close to the covalent radii sum [2.2751(11) and 2.2804(9) Å for **6** and **7**, respectively; Σr_{cov}(S, Pt) = 2.30 Å] [20] and are similar to the reported for a Pt^{IV} complex also containing a mixed donor N_2S ligand [2.281 Å] [21]. Due to the S→Pt coordination the eight-membered ring [$\boldsymbol{D}$(C$_2$N)$_2$M] displayed a boat-boat conformation.

3.3.2. Crystalline structures of **1**–**7**

All complexes displayed several noncovalent interactions in the crystalline state mainly due to the presence of hydrogen atoms covalently linked to electronegative nitrogen atoms, besides to the presence of aromatic rings and solvent molecules. To describe the intermolecular interactions based on hydrogen bonding, we used the graph analysis approach [22]. In all complexes the interatomic distances N–Cl ranged from 3.272 to 3.532 Å; these distances are close to the van der Waals radii sum [Σr_{vdW}(N, Cl) = 3.30 Å]. In the Figs. 4–6 are depicted some relevant hydrogen bond networks, with the corresponding graph descriptors.

Complexes [Pd{κ^2*N*-(NH$_2$-C$_6$H$_4$)$_2\boldsymbol{D}$}Cl$_2$]·*solvent* [$\boldsymbol{D}$ = O (**1**·DMSO), S (**3**·MeCN)] display similar hydrogen-bond networks based on

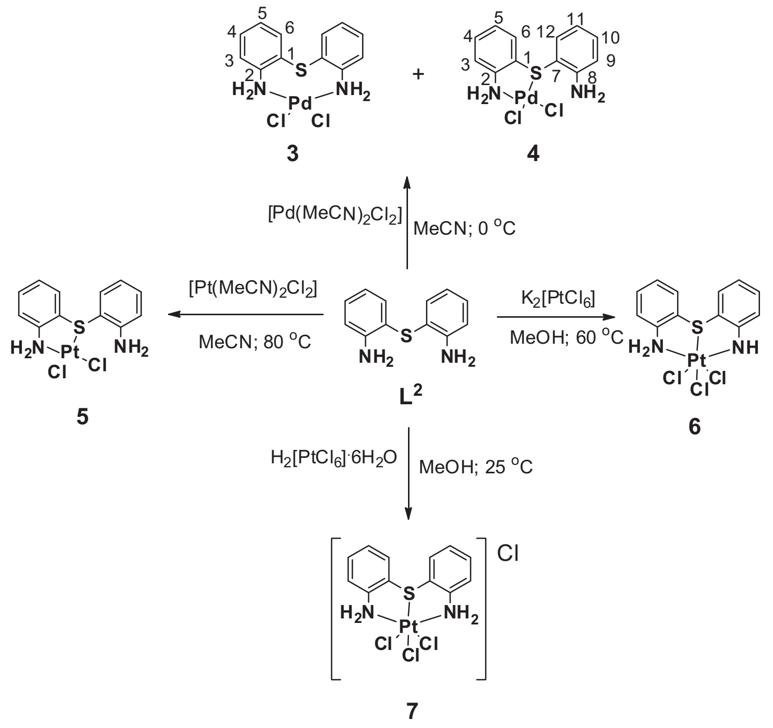

Scheme 2. Synthesis of the complexes of Pd and Pt derived from **L^2** (Numbering scheme for NMR is shown).

Table 1
Selected crystallographic data for **1**–**7**.

	1	**2**	**3**	**4**	**5**	**6**	**7**
Formula	$C_{14}H_{18}N_2O_2SCl_2Pd$	$C_{15}H_{18}N_2O_2Cl_2Pt$	$C_{14}H_{15}N_3SCl_2Pd$	$C_{12}H_{12}N_2SCl_2Pd$	$C_{13.5}H_{15}N_2O_{0.5}SCl_2Pt$	$C_{15}H_{17}N_2OSCl_3Pt$	$C_{15}H_{18}N_2OSCl_4Pt$
Formula weight	455.66	524.30	434.65	393.60	511.33	574.80	611.26
Crystal size (mm)	0.19 × 0.17 × 0.08	0.27 × 0.08 × 0.04	0.28 × 0.09 × 0.08	0.15 × 0.15 × 0.02	0.36 × 0.27 × 0.20	0.4 × 0.09 × 0.01	0.15 × 0.12 × 0.03
Crystal system	monoclinic	tetragonal	triclinic	monoclinic	monoclinic	triclinic	triclinic
Space group	$P2_1/c$	$I{-}4$	$P\bar{1}$	$P2_1/n$	$P2_1/n$	$P\bar{1}$	$P\bar{1}$
a (Å)	9.27877(16)	17.16260(18)	8.9725(2)	14.5945(5)	14.7427(2)	9.4165(2)	9.6727(3)
b (Å)	11.1953(2)	17.16260(18)	9.4016(2)	6.4110(3)	6.72165(10)	10.4431(3)	10.1370(3)
c (Å)	17.0552(4)	12.1175(2)	10.4623(2)	16.1332(5)	15.9629(2)	11.3179(2)	10.7563(3)
α (°)	90.00	90.00	86.7280(19)	90.00	90.00	111.979(2)	87.371(2)
β (°)	96.5291(18)	90.00	77.473(2)	96.900(3)	95.9503(14)	97.2139(19)	74.700(2)
γ (°)	90.00	90.00	77.552(2)	90.00	90.00	108.376(2)	79.133(2)
V (Å^3)	1760.17(6)	3569.27(9)	841.24(4)	1498.58(10)	1573.33(4)	941.20(4)	999.01(5)
Z	4	8	2	4	4	2	2
D_{calc} (Mg m^{-3})	1.719	1.951	1.716	1.745	2.159	2.028	2.032
μ (mm^{-1})	1.483	17.526	1.540	1.717	9.383	18.933	19.086
$F(000)$	912.0	2000.0	432.0	776.0	968.0	548.0	584.0
GOF on F^2	1.060	1.069	1.057	1.088	1.088	1.045	1.048
T (K)	295	295	295	295	295	295	295
2θ range (°)	6.02–52.6	7.28–147.2	5.78–52.74	6.84–52.74	6.58–52.74	8.768–144.194	8.52–148.96
Reflections collected	27936	19766	30923	22110	50009	34123	24731
Unique reflections	3566	3540	3430	3048	3192	3678	4081
Absorption correction	patterson	direct	direct	direct	direct	direct	direct
Independent reflections (R_{int})	0.0297	0.0651	0.0495	0.0507	0.0434	0.0622	0.0291
R_1, wR_2 [$I > 2\sigma(I)$]	0.0217, 0.0458	0.0357, 0.0854	0.0293, 0.0712	0.0256, 0.0474	0.0165, 0.0369	0.0286, 0.0705	0.0262, 0.0625
R_1, wR_2 [all data]	0.0287, 0.0488	0.0396, 0.0889	0.0400, 0.0769	0.0397, 0.0501	0.0202, 0.0385	0.0327, 0.0732	0.0290, 0.0643
Largest residuals (e Å^{-3})	0.30/−0.34	1.12/−0.57	0.71/−0.39	0.34/−0.34	1.26/−0.59	1.81/−0.87	1.65/−0.90

N–H–Cl interactions despite the different nature of both ***D*** atoms and crystallization solvents. The molecules of **1** displayed in the left part of the Fig. 5 are related by a twofold screw axis along *b* (space group $P2_1/c$) while the molecules of **3** are related by crystallographically distinct inversion centers (right; $P\bar{1}$). Both compounds display a characteristic topological element that consist of chains of rings, where the palladium acts as a "linker"; this chain was observed at the binary level and can be described

Table 2
Selected bond lengths [Å] and angles [°] for complexes **1**–**7**.

Compound	**1**·DMSO	**2**·Me_2CO	**3**·MeCN	4	**5**·Me_2CO	**6**·Me_2CO	**7**·Me_2CO
M	Pd	Pt	Pd	Pd	Pt	Pt	Pt
D	O	O	S	S	S	S	S
C(2)–N(1)	1.434(3)	1.452(11)	1.439(4)	1.452(3)	1.464(4)	1.372(7)	1.455(5)
C(8)–N(2)	1.440(3)	1.451(12)	1.431(4)	1.392(4)	1.395(5)	1.449(6)	1.459(5)
C(1)–*D*	11.392(3)	1.393(11)	1.787(3)	1.786(3)	1.784(3)	1.785(5)	1.787(4)
C(7)–*D*	1.397(3)	1.391(13)	1.789(3)	1.783(3)	1.792(3)	1.792(5)	1.787(4)
C(7)–C(8)	1.385(3)	1.414(12)	1.388(4)	1.399(4)	1.399(4)	1.382(7)	1.383(6)
C(1)–C(2)	1.385(3)	1.360(13)	1.390(4)	1.367(4)	1.381(5)	1.403(7)	1.381(6)
N(1)–M	2.052(2)	2.072(7)	2.070(3)	2.032(2)	2.031(3)	2.015(4)	2.062(3)
N(2)–M	2.058(2)	2.047(7)	2.081(3)	–	–	2.063(4)	2.069(3)
M–S(1)	–	–	–	2.2603(7)	2.2390(8)	2.2751(11)	2.2804(9)
M–Cl(1)	2.2961(6)	2.286(2)	2.2962(9)	2.2967(7)	2.3169(8)	2.3561(12)	2.3125(9)
M–Cl(2)	2.2992(6)	2.299(2)	2.2990(8)	2.2988(7)	2.3102(8)	2.3165(13)	2.3060(8)
M–Cl(3)	–	–	–	–	–	2.3222(12)	2.3255(10)
C(2)–N(1)–M	111.57(15)	111.8(5)	109.77(19)	116.4(2)	115.79(19)	115.7(3)	113.6(2)
C(8)–N(2)–M	115.81(15)	116.1(6)	117.8(2)	–	–	114.1(3)	113.5(2)
C(1)–S(1)–M	–	–	–	98.85(9)	99.49(11)	97.40(17)	97.55(13)
C(2)–C(1)–D	117.19(19)	118.0(8)	120.5(2)	118.70(19)	118.2(2)	116.0(4)	119.1(3)
C(8)–C(7)–D	117.49(19)	117.5(8)	121.5(2)	116.0(2)	115.9(2)	119.8(3)	119.6(3)
C(1) *D*–C(7)	115.91(17)	115.3(7)	98.51(13)	102.54(13)	102.01(15)	103.4(2)	103.39(17)
N(1)–M–N(2)	90.51(9)	90.6(3)	91.19(13)	–	–	86.95(16)	91.02(12)
N(1)–M–S(1)	–	–	–	86.70(8)	87.34(8)	85.92(12)	87.30(9)
Cl(1)–M–Cl(2)	92.01(2)	91.64(10)	91.99(3)	92.49(3)	92.41(3)	93.38(5)	92.04(4)
Cl(1)–M–Cl(3)	–	–	–	–	–	92.37(5)	91.41(4)
Cl(2)–M–Cl(3)	–	–	–	–	–	92.76(5)	92.06(4)
S(1)–M–Cl(3)						175.61(5)	177.18(3)

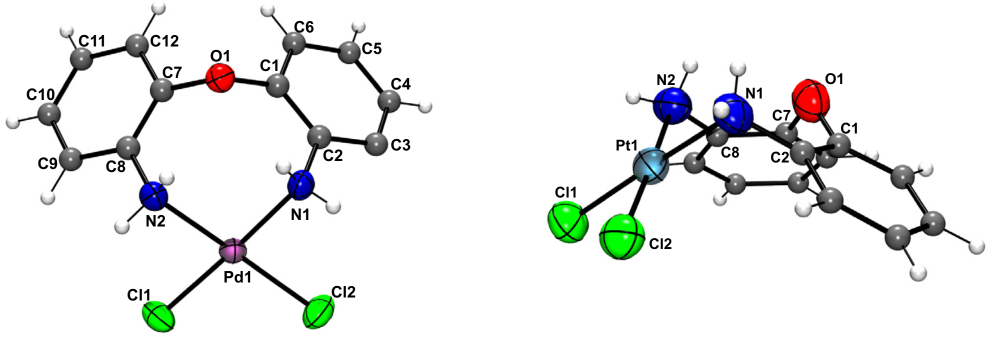

[Pd{κ^{2}N-(NH_2-C_6H_4)$_2$O}Cl_2]•DMSO (**1**•DMSO) Pt{κ^{2}N-(NH_2-C_6H_4)$_2$O}Cl_2]•Me_2CO (**2**•Me_2CO)

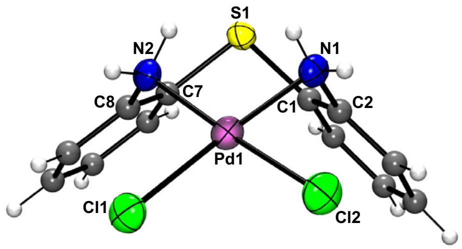

[Pd{κ^{2}N-(NH_2-C_6H_4)$_2$S}Cl_2]•MeCN (**3**•MeCN)

Fig. 2. Molecular drawings of complexes **1**, **2**, and **3** containing a κ^2*N* dicoordinate mode of the corresponding diaminic ligand (Thermal ellipsoids for non-carbon atoms at 50%; solvent molecules of crystallization have been omitted).

as $C_2^2(8)[R_2^2(8)]$. The platinum analog **2** also displays N–H–Cl interactions that result in tetrameric associations related by a fourfold rotoinversion axis along *c* (Fig. 6 top; space group *I*–4); in this compound the acetone molecules are also related by a *bar*-4 axis (Fig. 6, bottom). A relevant hydrogen bond pattern observed in **2** is a $R_2^2(8)$ ring at a unitary level, quite similar to the observed in compounds **1** and **3**.

Both [**M**{κ*N*,κ*S*-(NH_2-C_6H_4)$_2$S}Cl_2] complexes [**M** = Pd (**4**); Pt (**5**)] belong to the $P2_1/n$ space group; the presence of an acetone molecule in the Pt complex increases the cell volume by 75 Å^3 (5%) and, more remarkable, does not interfere with the formation of a chain of molecules along the *b* axis, which can be described by the binary level descriptor $C_1^2(4)$. Moreover, in both compounds is observed the same unitary level descriptors for the two rings

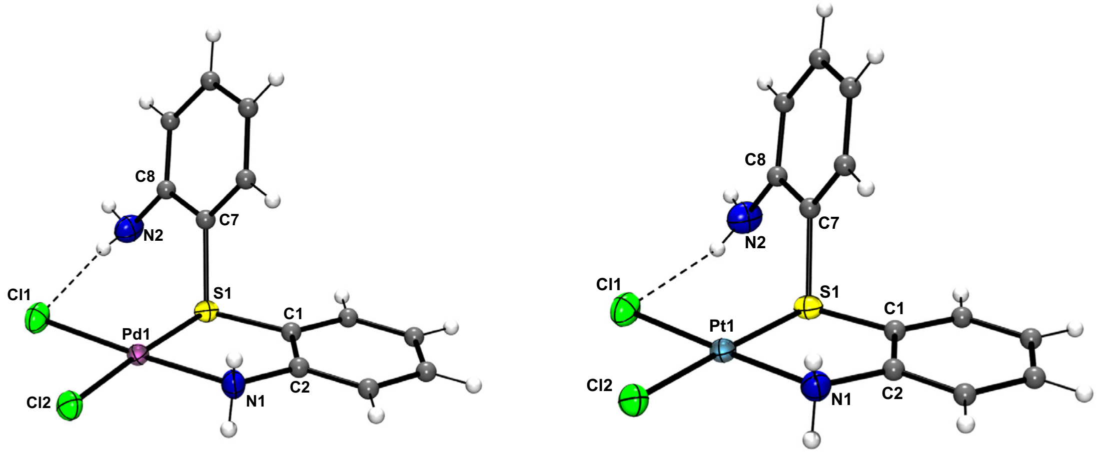

[Pd{κN,κS-$(NH_2-C_6H_4)_2S$}Cl_2] (**4**) [Pt{κN,κS-$(NH_2-C_6H_4)_2S$}Cl_2]•Me_2CO (**5**•Me_2CO)

Fig. 3. Molecular drawings of complexes **4** and **5** containing a κ*N*,κ*S* dicoordinate mode of the $\mathbf{L^2}$ ligand (Thermal ellipsoids for non-carbon atoms at 50%; acetone molecule of crystallization has been omitted).

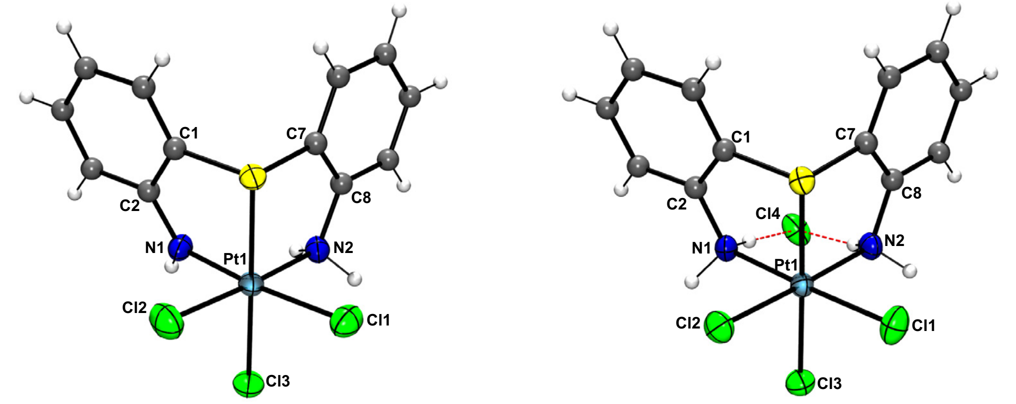

[Pt{κ^2N,κS-$(NH_2-C_6H_4)S(NH-C_6H_4)$}$Cl_3$]•$Me_2CO$ (**6**•Me_2CO) [Pt{κ^2N,κS-$(NH_2-C_6H_4)_2S$}Cl_3]Cl•Me_2CO (**7**•Me_2CO)

Fig. 4. Molecular drawings of complexes **6** and **7** containing a κ^2*N*,κ*S* tricoordinate mode of the $\mathbf{L^2}$ ligand (Thermal ellipsoids for non-carbon atoms at 50%; acetone molecules of crystallization have been omitted).

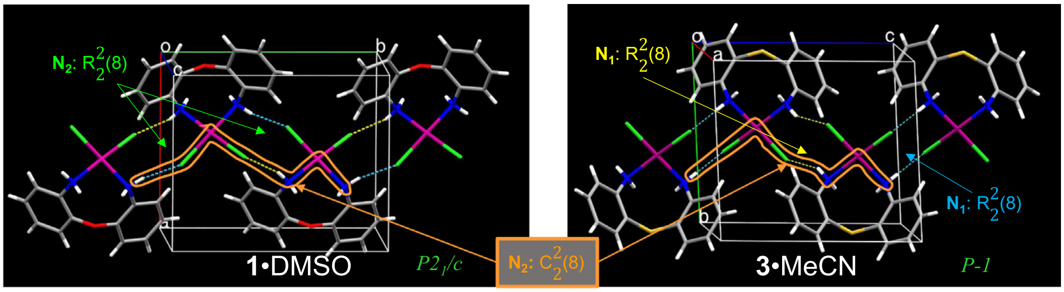

Fig. 5. Hydrogen-bond networks in complexes **1**·DMSO and **3**·MeCN containing a κ^2*N* dicoordinate mode of the corresponding diaminic ligand (Solvent molecules of crystallization have been omitted).

(showed in blue and yellow color in the Fig. 7). The complexes also display centrosymmetric **M**–**M** intermolecular dimeric interactions in a head–tail fashion; with distances of 3.340 and 3.356 Å for **4** and **5**, respectively; these interactions are similar to the van der Waals radii sum [Σr_{vdW}(Pd, Pd) = 3.26 Å; (Pt, Pt) = 3.44 Å]. Beside to these **M**–**M** interactions, there are also Cl–S interactions shorter than the van der Waals radii sum [3.347 Å (in **4**) and 3.417 Å (in **5**); Σr_{vdW}(Cl, S) = 3.55 Å]; the importance of this halogen bonding has been recognized as an important tool to enhance self-assembly processes [23]. Overall, it is reasonable to consider that the

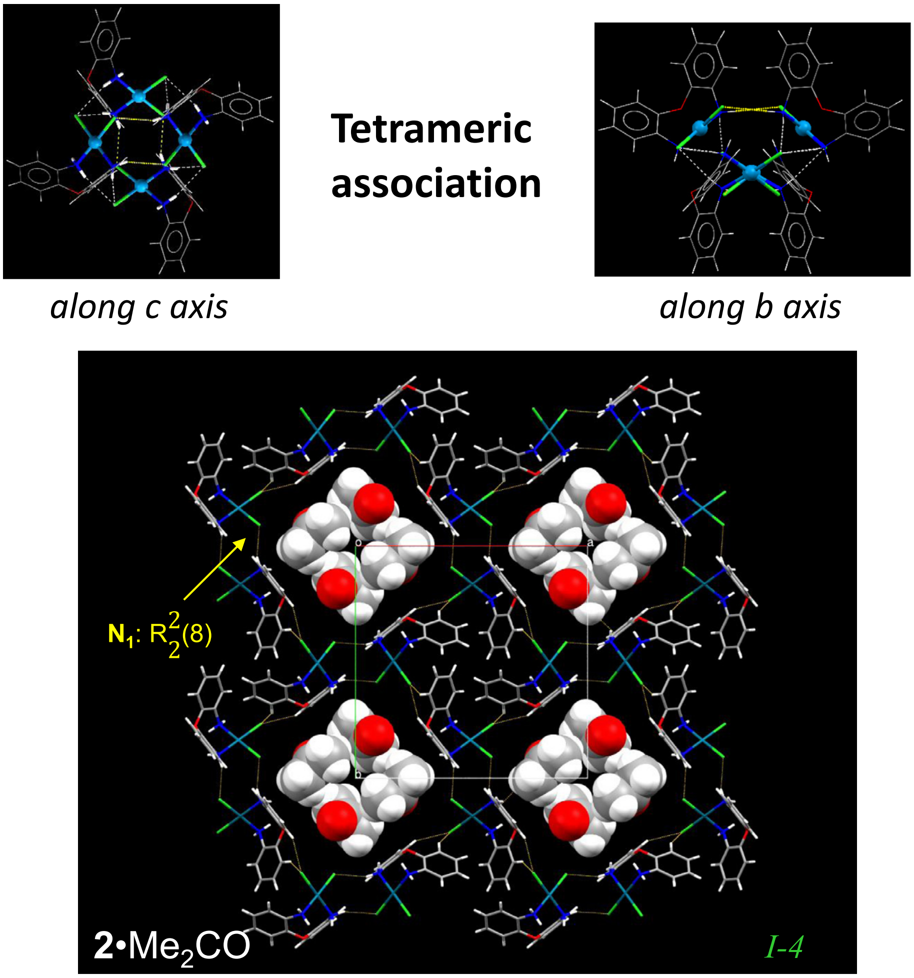

Fig. 6. Hydrogen-bond networks in complex **2**·Me$_2$CO containing a κ^2*N* dicoordinate mode of the diaminic ligand **L^1**.

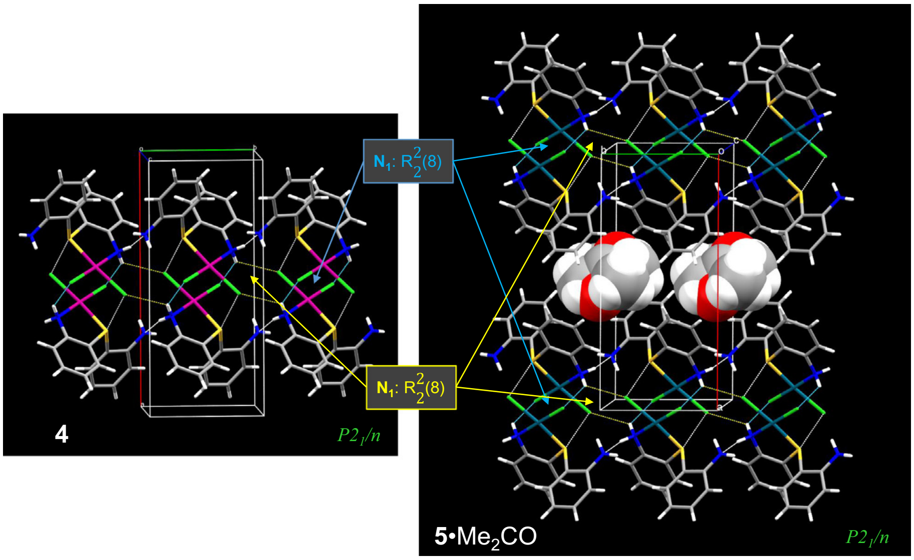

Fig. 7. Hydrogen-bond networks in complexes **4** and **5**·Me$_2$CO containing a κ*N*,κ*S* dicoordinate mode of the **L^2** ligand.

hydrogen- and halogen bonding cooperative interactions are the responsible for retaining the similar arrangements of the molecules [**M**{κ*N*,κ*S*-(NH$_2$-C$_6$H$_4$)$_2$S}Cl$_2$] above described.

Lastly, the six-coordinate platinum(IV) complexes displayed similar rings related by an inversion center at both unitary and binary levels (Fig. 8), in spite of the distinct nature of the acceptor atoms linking the Pt^{IV} coordination entities (oxygen in **6** respect to chloro in **7**) as well as their different type of coordination entity (neutral versus ionic type).

3.4. NMR spectra

The characterization in solution of the ligands $\mathbf{L^1}$ and $\mathbf{L^2}$ and the complexes **1**, **2**, **5**, and **7** by means of ^1H and $^{13}C\{^1H\}$ NMR at room temperature was carried out in DMF–acetone-d_6 mixtures (1:2), for **3** and **4** was used DMF-d_7, while characterization of **6** was determined in an acetone-d_6 solution. Chemical shifts and the assignment of the proton and carbon atoms of **1**–**7** are listed in the Section 2. For $\mathbf{L^1}$, the ^1H–^1H NOESY experiment showed a correlation of the $-NH_2$ protons at 4.85 ppm with a multiple signal at 6.85 ppm; this signal is due to the overlapping of the individual H3 and H4 protons; for $\mathbf{L^2}$ the ^1H–^1H NOESY experiment carried out in DMSO-d_6 showed a correlation between the $-NH_2$ protons at 5.30 ppm and a signal displayed as a double of doublets at 6.72 ppm assigned to the H3 proton.

^1H NMR spectra of the complexes **1** and **2** displayed three sets of signals for both magnetically equivalent phenyl rings. From the ^1H data the formation of eight–membered chelate rings containing the ligand $\mathbf{L^1}$ in a κ^2N bidentate coordinating mode is proposed. This proposal was confirmed with the analysis of the $^{13}C\{^1H\}$ NMR spectra, where just six signals were observed in the region of the aromatic carbon atoms, (Fig. 3S, see Supplementary Material).

In the NMR spectra, the complexes **3** and **4** were observed as a mixture of linkage isomers in a 30:70 ratio; moreover, if pure crystals of either **3** or **4** are dissolved in a DMF–acetone-d_6 mixture, they gradually reach the above ratio. When this solution was heated to 50 °C, the signals displayed coalescence; when the solution was cooled to room temperature, the previously observed ratio of the isomers is once again reached (Fig. 4S in the Supplementary Material). Complex **3** is the minor product and displayed an ABCD pattern for both phenyl rings with a κ^2N bidentate coordinating mode of the ligand $\mathbf{L^2}$. On the other hand, the major complex **4** displayed two ABCD patterns for each magnetically and chemically non-equivalent phenyl rings, corresponding to the formation of a five-membered chelate ring. These facts were also ratified with the $^{13}C\{^1H\}$ NMR data where six and twelve signals were observed for **3** and **4**, respectively (Fig. 5S, see Supplementary Material). Overall, it is suggested that in solution these linkage isomers coexist in equilibrium at room temperature, Fig. 9.

Complex **5** displayed a similar spectroscopic behavior to the analogous **4**, with a five-membered chelate ring assigned in solution, (Figs. 6S and 7S, see Supplementary Material). The ^1H spectra of **6** and **7** exhibited an ABCD pattern for both phenyl groups. From the analysis, we proposed for complexes **6** and **7** a $\kappa^2N,\kappa S$ tridentate coordinating mode of the ligand $\mathbf{L^2}$ toward the Pt^{IV}; this proposal agrees with the X-ray diffraction data of **6** and **7** (*vide supra*).

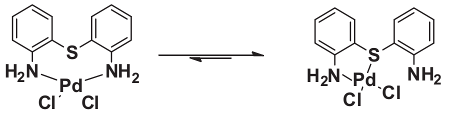

3 (κ^2N mode)

4 ($\kappa N\kappa S$ mode)

Fig. 9. Equilibrium in solution for **3** and **4** at room temperature.

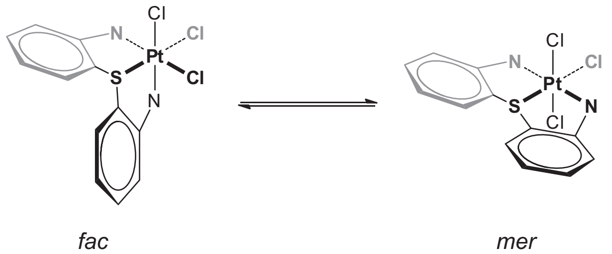

Fig. 10. *Fac–mer* geometric isomerism in solution proposed for **6** and **7** (Only the coordination entity is shown for each complex; the hydrogen atoms attached to nitrogen atoms have been omitted for the sake of clarity).

^1H NMR spectra of Pt^{IV} complexes **6** and **7** at room temperature displayed the aromatic protons as broad signals, in particular the triplet assigned to the H4 and H10 protons was observed as a very broad signal. At 40 °C, the ^1H spectrum of **7** showed sharp signals whereas **6** showed decomposition products. The $^{13}C\{^1H\}$ spectra of **6** and **7** displayed similar results at both temperatures; i.e., we observed a reduced number of signals for both complexes at room temperature and the expected number of signals in the case of **7** and decomposition products for **6** at 40 °C. The observation at room temperature of broad signals in **6** and **7** is attributed to the existence in solution of both *mer–fac* conformers (Fig. 10), an observation that has been reported for some metallic analogues of $\mathbf{L^1}$ [24,25].

We analyzed the variations of the chemical shifts ($\Delta\delta$) for the *ipso*-C1 atom; in the κ^2N complexes **1** and **2** the low-frequency variation respect to $\mathbf{L^1}$ was of 8.1 and 7.6 ppm. In the case of the $\kappa N,\kappa S$ complexes **4** and **5** the same C1 displayed $\Delta\delta$ values of 15.7 and 17.8 ppm at high frequencies, respectively. The larger values of $\Delta\delta$ in **4** and **5** could be attributed to the combination of two factors: an electronic factor due to the greater affinity of the sulfur donor atom to bind the $\mathbf{M^{II}}$ center and a structural factor related with the annular tension originated by the five–membered chelate ring.

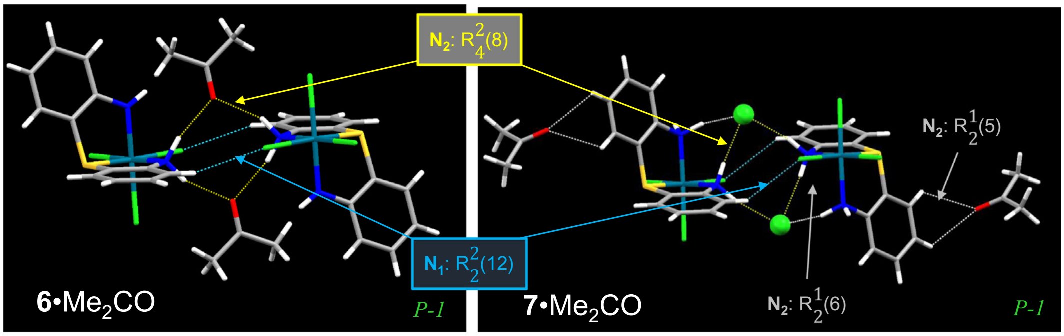

Fig. 8. Hydrogen-bond networks in complexes $\mathbf{6}\cdot Me_2CO$ and $\mathbf{7}\cdot Me_2CO$ containing a $\kappa^2N,\kappa S$ tricoordinate mode of the $\mathbf{L^2}$ ligand.

4. Conclusion

New complexes of palladium and platinum containing $\{(NH_2\text{-}C_6H_4)_2\boldsymbol{D}\}$ ligands [$\boldsymbol{D}$ = O (**L**$^{\mathbf{1}}$), S (**L**$^{\mathbf{2}}$)] have been synthesized. The analysis of the molecular structures revealed three types of coordination modes of the diamino ligands toward the central atom **M**^{II} (**M** = Pd, Pt). A κ^2N mode was observed in **1** and **2** when a hard donor oxygen atom is present in the ligand **L**$^{\mathbf{1}}$; in both cases the oxygen atom was not involved in any transannular intramolecular bonding. A distinct situation was observed in the case of the ligand **L**$^{\mathbf{2}}$. In the complexes containing a Pd^{II} cation (**3** and **4**) were observed two κ^2N and $\kappa N,\kappa S$ modes by means of NMR studies in solution as well as by single crystal X-ray studies; meanwhile with platinum ion acting as central atom (**5–7**) the ligand just displayed modes where the sulfur atom is bound to Pt^{II} or Pt^{IV}, properly $\kappa N,\kappa S$ and $\kappa^2N,\kappa S$ modes. Overall, these different binding modes are consistent with the wide coordination versatility of the ligands **L**$^{\boldsymbol{n}}$.

In the solid state, the presence of several N–H functions enhanced the formation of supramolecular associations. There are remarkable tendencies in the networks, in spite of the distinct solvent molecules contained in each cell. The **1**·DMSO, **2**·Me_2CO, and **3**·MeCN complexes displaying κ^2N coordination modes also displayed similar associations based on N–H–Cl interactions described by $R_2^2(8)$. Both isostructural $\kappa N,\kappa S$ complexes **4** and **5**·Me_2CO are associated by N–H–Cl, Cl–S, and **M**–**M** interactions despite of the presence of an acetone molecule in the cell of **5**. The importance of the networks based on N–H–Cl interactions is emphasized in the crystal structures of the Pt^{IV} neutral **6**·Me_2CO and ionic **7**·Me_2CO complexes; nevertheless their distinct nature, both displayed the same type of rings motifs $R_2^2(12)$ and $R_4^2(8)$ at the unitary and binary levels, respectively, with quite different acceptors such as oxygen (from Me_2CO) or chloride anion.

Acknowledgements

We thank Dr. Diego Martínez Otero (UNAM) for his assistance in X-ray crystallography. UHB fully acknowledge the scholarship from CONACYT. This research was supported by CONACYT (Project 81003).

Appendix A. Supplementary data

CCDC 1030380–1030386 contain the supplementary crystallographic data for **1**–**7**. These data can be obtained free of charge via http://www.ccdc.cam.ac.uk/conts/retrieving.html, or from the Cambridge Crystallographic Data Centre, 12 Union Road, Cambridge CB2 1EZ, UK; fax: (+44) 1223-336-033; or e-mail: deposit@ccdc.cam.ac.uk. Supplementary data associated with this article can be found, in the online version, at http://dx.doi.org/10.1016/j.poly.2015.02.004.

References

[1] R.R. Schrock, R. Baumann, S.M. Reid, J.T. Goodman, R. Stumpf, W.M. Davis, Organometallics 18 (1999) 3649.
[2] G.J.P. Britovsek, V.C. Gibson, O.D. Hoarau, S.K. Spitzmesser, A.J.P. White, D.J. Williams, Inorg. Chem. 42 (2003) 3454.
[3] A. Panunzi, F. Giordano, I. Orabona, F. Ruffo, Inorg. Chim. Acta 358 (2005) 1217.
[4] R.J. van Haaren, P.H. Keeven, L.A. van der Veen, K. Goubitz, G.P.F. Strijdonck, H. Oevering, J.N.H. Reek, P.C.J. Kamer, P.W.N.M. van Leeuwen, Inorg. Chim. Acta 327 (2002) 108.
[5] J.G. Alvarado-Rodríguez, S. González-Montiel, N. Andrade-López, J.A. Cogordan, L.L. Lima-Ortiz, Polyhedron 29 (2010) 2283.
[6] D. Martínez-Otero, J.G. Alvarado-Rodríguez, J. Cruz-Borbolla, N. Andrade-López, T. Pandiyan, R. Moreno-Esparza, M. Flores-Alamo, J. Cantillo-Castillo, Polyhedron 33 (2012) 367.
[7] S. González-Montiel, B. Flores-Chávez, J.G. Alvarado-Rodríguez, N. Andrade-López, J.A. Cogordan, Polyhedron 28 (2009) 467.
[8] S. González-Montiel, J.G. Alvarado-Rodríguez, N. Andrade-López, Eur. J. Inorg. (2006) 3762.
[9] H. Cui, R. Goddard, K.-R. Pörschke, A. Hamacher, M.U. Kassack, Inorg. Chem. 53 (2014) 3371.
[10] U. Hernández-Balderas, G. Rodríguez-García, N. Andrade-López, J.G. Alvarado-Rodríguez, R. Moreno-Esparza, M. Flores-Alamo, Polyhedron 36 (2012) 104.
[11] J.R. Pioquinto-Mendoza, D.G. Olvera-Mendoza, N. Andrade-López, J.G. Alvarado-Rodríguez, R. Moreno-Esparza, M. Flores-Álamo, Coord. Chem. 66 (2013) 2477.
[12] J.R. Pioquinto-Mendoza, D. Martínez-Otero, N. Andrade-López, J.G. Alvarado-Rodríguez, V. Salazar-Pereda, G. Sánchez-Cabrera, F.J. Zuno-Cruz, Polyhedron 50 (2013) 289.
[13] Yu.V. Kokunov, Yu.E. Gorbunova, V.V. Kovalev, Russ. J. Inorg. Chem. 54 (2009) 1678.
[14] C.J. Mathews, P.J. Smith, T. Welton, J. Mol. Catal. A. Chem. 206 (2003) 77.
[15] Oxford Diffraction, CRYSALIS software system, version 1.171.33.31. Oxford Diffraction Ltd., Abingdon, UK, 2009.
[16] O.V. Dolomanov, L.J. Bourhis, R.J. Gildea, J.A.K. Howard, H. Puschmann, J. Appl. Crystallogr. 42 (2009) 339.
[17] G.M. Sheldrick, Acta Crystalogr., Sect. A 64 (2008) 112.
[18] J.F.K. Wilshire, Aust. J. Chem. 41 (1998) 995.
[19] C.C. Price, G.W. Stacy, Org. Syn. Coll. 3 (1955) 667.
[20] W.W. Porterfield, Inorganic Chemistry: A Unified Approach, second ed., Academic Press Inc., USA, 1993. p. 214.
[21] U. Heinzel, R. Mattes, Polyhedron 10 (1991) 19.
[22] J. Bernstein, R.E. Davis, L. Shimoni, N.-L. Chang, Angew. Chem. Int. Ed. Engl. 34 (1995) 1555.
[23] P. Metrangolo, G. Resnati, Chem. Eur. J. 7 (2001) 2511.
[24] D.D. Grafs, W.M. Davis, R.R. Schrock, Organometallics 17 (1998) 5820.
[25] L.-C. Liang, R.R. Schrock, W.M. Davis, Organometallics 19 (2000) 2526.